A Bifocal Arrangement for Reflected Caustics for the Investigation of the Domain of Dominance of Asymptotic Elastic Fields in Dynamic Fracture

SRIDHAR KRISHNASWAMY*, ARES ROSAKIS* and G. RAVICHANDRAN**

*California Institute of Technology, Pasadena, CA 91125, USA

**University of California, San Diego, La Jolla, CA 92093, USA

ABSTRACT

The question of the domain of dominance of the plane-stress asymptotic elastic fields in dynamic fracture is addressed for the two cases of dynamically loaded stationary cracks as well as dynamically propagating cracks. The experiments reported in this work are on three-point bend, 4340 steel specimens loaded dynamically using a drop-weight tower. A new optical configuration is proposed which would allow for the simultaneous measurement of the apparent dynamic stress-intensity factor from two different regions around the crack-tip using the method of caustics. The results of the study indicate the importance of three-dimensional and transient effects in the interpretation of optical measurements.

KEYWORDS

Dynamic stress-intensity factor; asymptotic fields; bifocal caustics.

INTRODUCTION

The primary focus of dynamic fracture mechanics of nominally brittle materials has been the determination of the dynamic fracture toughness for initiation and its dependence on loading rate as well as the study of the propagation toughness (K_{ID}) and its possible dependence on parameters such as crack velocity ($\dot{a}$), acceleration and temperature. Extensive experimental effort has gone into these tasks over the past two decades. The principal tools for investigation have been the method of caustics and photo-elasticity. Both these techniques require an *a priori* knowledge of the form of the near-tip stress or deformation fields. It has been the vogue to assume that the plane-stress dynamic stress-intensity factor field (the K_I^d-field) adequately approximates the stresses and displacements over some region around the crack-front. Based on this assumption of K_I^d-dominance, the endeavor thus far has been to experimentally obtain a measure of the dynamic stress-intensity factor (and hence fracture toughness) for rapidly propagating cracks. Using this approach,

some researchers (Kobayashi *et al.*, 1980, Rosakis *et al.*, 1984 and Zehnder, 1987) among others, have found that the dynamic fracture toughness depends in a one-to-one manner on the crack velocity. This is disputed by others (Kobayashi *et al.*, 1978 and Ravi-Chandar *et al.*, 1984) who do not find support for such a relation. In addition, Takahashi *et al.*, (1987) have argued for an acceleration dependence of the dynamic fracture toughness and Kalthoff (1983) has reported that there is a sytematic specimen dependence of the dynamic fracture toughness. Note that in many of above works, the conclusions reached are on the basis of observed variatiors in the stress-intensity factor of between 20-60%.

The view taken here is that it is possible that the lack of an underlying K_I^d-dominant field presumed in the interpretation of the experiments might be the cause of the observed acceleration and specimen depencence of the dynamic fracture toughness. This could also have a bearing on the prevalent diverging views regarding the uniqueness of the $K_{ID} - \dot{a}$ relation. It is felt that this issue needs to be addressed. In this paper, the question of the adequacy of the K_I^d-field as a characterizer of the near-tip fields is evaluated for the case of a dynamically loaded three-point bend specimen. This question arises because it is becoming increasingly clear that the near-tip fields deviate substantially from the assumed plane-stress field because of three-dimensional effects. In addition, the asymptotic K_I^d-field is expected to become progressively more inaccurate away from the crack-tip even in a two-dimensional dynamic setting. Thus, a K_I^d-dominant region, if it were to exist, must be an annulus around the crack-tip. The corresponding issue for the static case has been investigated by Rosakis *et al.*, (1986) where the near-tip three-dimensionality was seen to be confined to within a radial distance of one-half plate thickness. The issue of K_I^d-dominance in the dynamic case is investigated in this paper by means of the method of caustics in reflection used in conjunction with a proposed bifocal high-speed camera set-up as discussed below.

THE METHOD OF CAUSTICS

A detailed exposition of the theory of the method of caustics can be found in Manogg (1964) and Rosakis *et al.*, (1985). Here only a brief outline of the method of caustics in reflection will be presented. A schematic diagram of the experimental method is shown in Fig. 1. A collimated laser beam is incident on a polished, optically flat fracture specimen and the reflected light is collected and imaged in a camera. The camera is set to focus on a virtual object plane at a distance z_0 behind the specimen. When the specimen is loaded, its surface gets deformed by, say, $x_3 = -f(x_1, x_2)$, where (x_1, x_2) are points on the specimen. Due to this deformation, a light ray incident at a point (x_1, x_2) on the specimen gets mapped to a point (X_1, X_2) on the virtual object plane of the camera. The mapping can be shown to be given by (Rosakis *et al.*, 1985)

$$\underline{X} \approx \underline{x} - 2z_0 \nabla f \tag{1}$$

where it has been assumed that $z_0 \gg max\,|f(x_1, x_2)|$ which is true for the all the experiments reported in this work. For caustics by reflection, $f(x_1, x_2)$ is the out-of-plane displacement field $u_3(x_1, x_2)$ which, for thin elastic plates of uniform thickness h, is given by

$$u_3 = \frac{-\nu h}{2E}(\sigma_{11} + \sigma_{22}), \tag{2}$$

where E is the Young's modulus and ν is Poisson's ratio. Note that relation (2) is a consequence of assuming that plane-stress conditions prevail throughout the thin plate.

Caustics in Elastodynamic Fracture

Consider a fracture specimen made of a linear elastic, isotropic solid subject to mode-I, generalized plane-stress conditions. Suppose that inertial effects need to be included either due to dynamic loading of a stationary crack or due to rapid crack propagation. Based on an asymptotic solution (Freund *et al.*, 1974), it is commonly assumed that the near-tip stress field with reference to an $(r - \theta)$ polar coordinate system translating with the crack-tip is given by

$$\sigma_{\alpha\beta} \approx \frac{K_I^d(t)}{\sqrt{2\pi r}}\,\Sigma_{\alpha\beta}(\theta, \dot{a}) \qquad b < r < a, \tag{3}$$

where $K_I^d(t)$ is a time-dependent dynamic stress-intensity factor and $\Sigma_{\alpha\beta}$ are known universal functions of θ and crack velocity $\dot{a}$. This expression is supposed to hold in an annulus around the crack-tip given by $b < r < a$ where 'b' is dictated by the extent of the three-dimensional zone surrounding the crack-tip and 'a' is a relevant in-plane length and may be dictated by the transient nature of the loading. A region where (3) holds is called a K_I^d-dominant region. If the out-of plane displacement field corresponding to (2) and (3) is subjected to the caustic mapping (1), a characteristic shadow-spot surrounded by a bright caustic (see Fig. 2) is seen. The transverse diameter D of the caustic can be shown (Rosakis, 1980) to be related to the instantaneous stress-intensity factor through

$$K_I^d = \frac{ED^{5/2}}{10.7 z_0 \nu h} F(\dot{a}) C(\alpha_l) \tag{4}$$

where $F(\dot{a})$ and $C(\alpha_l)$ are known functions of crack-velocity. For sufficiently small crack velocities ($\dot{a} < 0.3c_s$), the locus of points on the specimen that map onto the caustic (the initial-curve) is very nearly circular and its nominal radius can be approximated by (Rosakis, 1980)

$$r_0(t) = \left(\frac{3h\nu K_I{}^d(t) z_0}{2\sqrt{2\pi E}}\right)^{2/5} F(\dot{a})^{(-2/5)}. \tag{5}$$

The above equations in the limit $\dot{a} \to 0$ are also valid for the case of a dynamically loaded stationary crack. In a typical experiment, a high-speed camera would be used to obtain a time sequence of caustics from whose diameter $D(t)$, the stress-intensity factor, $K_I^d(t)$, would be computed using (4). From (5), one finds that $r_0(t) = \hat{r}_0(K_I^d(t), z_0, \dot{a})$ and as $K_I^d(t)$ varies with time in a dynamic experiment, the radius of the initial-curve would perforce change during the course of the experiment. Thus from the point of view of experiments, it is vital to know that relation (2) based on the plane-stress approximation together with the asymptotic expression (3) lead to a valid expression for the displacement field for at least the range of radii that the initial curve would cover during the event of interest.

To make matters a bit more explicit, suppose that during the event of interest (which could be the crack propagation phase of a test) the initial-curve radius is known from previous experience to vary in the region $r_{min} \le r_0 \le r_{max}$ for some choice of the object plane distance z_0. Also, since the domain of validity of (3) could in general be time-dependent as well, let 'b' and 'a' be such as to give the smallest annulus in which (2) holds for all times during the entire event of interest. Then, for a valid interpretation of the caustics, the inequalities $b < r_{min} \le r_0 \le r_{max} < a$ must be satisfied in order to have the initial-curve fall in a region of K_I^d-dominance.

The first attempts to address the issue of the validity of (3) are reported in Ravi-Chandar *et al.*, (1987). A series of tests was performed using the method of caustics in transmission

on identical specimens under identical stress-wave loading, varying from test to test only the object plane distance z_0. In this manner a range of initial-curve radii was scanned and since, presumably, the actual stress-intensity factor history $K_I^d(t)$ for the various tests must be identical, the apparent stress-intensity factors measured from caustics obtained from different object planes must also agree, at least for those times when the initial-curves fall within the region of K_I^d-dominance. The findings of Ravi-Chandar *et al.*, (1987) indicate that the assumption behind (3) might not be tenable. Since a substantial part of the dynamic fracture data extant in the literature has been obtained through the use of either photo-elasticity or the method of caustics, the ramifications of this result are potentially far-reaching and thus deserve more careful scrutiny.

In particular, it would be preferable to be able to obtain the apparent stress-intensity factor values from different initial-curves around the crack-tip for the same specimen at any given instant in time. While comparison of results across tests can be made with confidence for the loading regime of the experiments, it becomes more difficult in the crack propagating phase since small variations in the crack motion history could lead to large variations in the values for the measured stress-intensity factor. For example, Fig. 3a shows the stress-intensity factor history obtained through the method of caustics from a set of three different tests on identical specimens and for the same object plane distance z_0. Note that the scatter in these results is within the expected experimental error of about ±5% (as computed through an error analysis of (4)). The same, however, is not true for the propagating phase. As can be seen in Fig. 3b, the crack does not quite initiate at the same time even though the specimens were ostensibly identical and were subjected to essentially the same loading. The differences are possibly due to unavoidable minor variations in the crack-tip bluntnesses. Thus, the rather large variations seen in Fig. 3b arise not so much from experimental uncertainty as from the fact that the initiation times and, therefore, the subsequent propagation histories are different. It is in an attempt to avoid this problem that one would like to be able to obtain caustics from different initial-curves simultaneously from the same experiment. Here, an optical configuration that would allow for the *simultaneous* acquisition of dynamic caustics from *two* different object planes (and hence two different initial-curves) using only a *single* high-speed camera will now be discussed.

THE METHOD OF BIFOCAL CAUSTICS

A schematic of the optical set-up required to bring two different object planes simultaneously into focus in a single camera is shown in Fig. 4. The set-up entails the use of two beam-splitters and two mirrors by which two optical paths of different path lengths are established between the specimen and the high-speed camera. With reference to the figure, let the high-speed camera be set up to focus at a distance f from the camera lens. Along path(1) this would mean that the virtual object plane is located at distance z_{01} behind the specimen. Along path(2) however, by virtue of the increased length ($2L$) between the specimen and the camera lens, the object plane would now fall only at a distance $z_{02} = z_{01} - 2L$ behind the specimen. Thus the caustics obtained from the two paths would be from two different initial-curve radii. They could be made to appear on the film track of the high-speed camera either superposed or side by side. Fig. 5a shows a representative picture of bifocal caustics for the case of the dynamically loaded stationary crack. The superposition of the two images from the bifocal set-up was here so arranged as to have

the pairs of caustics (the two bright lines around the crack-tip) one slightly shifted with respect to the other. The smaller caustic corresponds to the smaller object plane distance (z_{02}) and the larger one to z_{01}. An example of bifocal caustics for the propagating case is shown in Fig. 5b.

For nomenclatural convenience, the pairs of dynamic caustics obtained by use of this bifocal high-speed camera will henceforth be referred to as 'bifocal caustics,' with the implicit understanding that such caustics are obtained from two different initial-curves on the same specimen at the same time. (There is, of course, a time delay of $2L/c$ because of the finiteness of the speed of light c, but this is negligible for values of L used in practice.) By changing the distance L from test to test or by changing the focal plane of the camera, one could of course scan various sets of initial-curves. The comparison of whether the apparent stress-intensity factors obtained from the bifocal caustics agree over some range of r_0 would however be done solely within each test for reasons stated earlier.

Results of the Bifocal Caustics Experiment

The tests were done on three-point bend AISI 4340 steel specimens 30.5cm long, 15.25cm wide, 1cm thick with an initial notch of about 3.8cm. The specimens were heat-treated as follows: (1) normalize at 1650°C for one hour and air-cool, (2) austenitize at 1550°C for one hour and oil-quench and (3) temper at 200°C for one hour and air-cool. One surface of each specimen was lapped and polished to give a highly reflective surface. The Dynatup 8100A drop-weight tower was used as the loading device. A rotating mirror high-speed camera in conjunction with an argon-ion pulse laser was used to record a time-sequence of bifocal caustics as described earlier. The details of specimen preparation and the experimental set-up may be found in Krishnaswamy (1988). The pairs of caustics obtained at each instant of time were analyzed as described earlier to get the apparent stress-intensity factor histories. Only representative preliminary results will be presented here. Fig. 6a shows the results for the uninitiated dynamically loaded crack for specimen $\alpha - 3$. The two apparent stress-intensity factors obtained from the diameters of the bifocal caustics pairs are shown as functions of time from impact. The object plane distances used in this experiment were z_{01} = 4.82m and z_{02} = 3.08m. The region of possible measurement uncertainty is indicated as vertical error bars. Fig. 6b is an alternate representation of the experimental results for specimen $\alpha - 3$. Here, the ratio of the two stress-intensity factors from the bifocal caustic pairs (K_{I1}^d/K_{I2}^d) is plotted as a function of time from impact. Also plotted as a function of time are the radii of the initial-curves for the two choices of object plane distance. It is seen that the apparent measured stress-intensity factor is not quite independent of the region from which the measurement is made. Indeed, differences greater than 40% are observed between the measured stress-intensity factors obtained from initial-curves whose radii vary by less than 20% of the plate thickness. Further, the larger measured stress-intensity factor corresponds to the larger object plane distance and hence larger initial-curve radius. Unlike the results of Rosakis *et al.*, (1986) for the static case, these differences persist even for $r_0/h \geq 0.5$.

A representative set of results for the crack propagation phase is shown in Fig. 7a,b. These are again time history plots of the two measured dynamic stress-intensity factors from the bifocal caustics pairs. The larger initial-curve is again seen to give a larger apparent stress-intensity factor. Differences of upto 30% in the measured values are seen

in these experiments. The initial-curve radii are almost always greater than one-half the specimen thickness during the crack-propagation phase. These differences, therefore, do not disappear for $r_o/h \geq 0.5$ during the propagation phase as well (unlike the static case).

DISCUSSION

The results of both the dynamically-loaded stationary crack and the dynamically propagating crack tests seem to imply that the *the apparent dynamic stress-intensity factor as measured by the method of caustics increases substantially with increasing initial-curve radius.* This means that the assumption that the plane-stress asymptotic field (2) is valid over this range of radius cannot be correct. That is, for the experiments considered, no sizeable region of K_I^d-dominance can be said to exist at least insofar as the surface displacements are concerned. The reasons for this are not difficult to identify. As suggested earlier, the interplay between three-dimensional effects and the transient nature of the loading is expected to be the major factor. This has since been confirmed by two- and three-dimensional elastodynamic simulations (upto the point of crack initiation) of the drop-weight tests which were undertaken in a companion study. The actual experimental boundary conditions were used in these simulations. The details of the simulations may be found in Krishnaswamy (1988) and are beyond the scope of this paper. Some pertinent results from the simulations, however, will be presented here. Figures 8a,b show the radial and angular variation of the free-surface out-of-plane displacements computed through a three-dimensional elastodynamic analysis. These are normalized by the corresponding plane-stress asymptotic values. It can be seen that there is no sizeable annulus around the crack-tip where the asymptotic field can be said to adequately model the three-dimensional out-of-plane displacements. In addition, the numerically simulated surface out-of-plane displacements were subjected to the caustic mapping (1) and a representative set of these is shown in Fig. 9a for a range of z_0's and one particular time in the simulation. If one were to relate the caustic diameters to the stress-intensity factor through (4), then the resulting values for the measured stress-intensity factor (shown for two times) are seen to vary quite substantially with increasing initial-curve radius as shown in Fig. 9b. Here, K_j is a measure of the stress-intensity factor as obtained from the finite-element simulation of the experiments. It is seen that the almost monotonically increasing K_{caus}/K_j vs r_o/h curve for the three-dimensional transient simulation case qualitatively captures essentially all the features observed experimentally. Thus, the apparent dynamic stress-intensity factor as measured by caustics would seem to increase with increasing initial-curve radii. Also note that unlike the results of Rosakis *et al.*, (1986), the variation of the measured stress-intensity factor persists even for $r_0/h \geq 0.5$.

As a parenthetical note, it is interesting that the variation in K_{I1}^d and K_{I2}^d – the two values for the dynamic stress-intensity factor as measured from pairs of bifocal caustics – turns out to be in quite good *quantitative* agreement with the results of Fig. 9b. That is, the ratio of K_{I1}^d to K_{I2}^d as obtained from experiments seem to be in close agreement with that obtained from Fig. 9b for the corresponding initial-curve radii. This can be seen in Fig. 10 where the numerically generated results of Fig. 13b are used to "scale" the results of one particular experiment. To do this, *assume* that the results of Fig. 9b (K_{caus}/K_j vs r_0/h) hold for the whole duration of the loading. The experimental data (corresponding to the two z_0's) shown in Fig. 10a can then be scaled, for each time, to the corresponding 'K_j' value by means of Fig. 9b. The resulting "scaled" dynamic stress-intensity factor histories

corresponding to the two z_0's are shown in Fig. 10b. It is seen that by this procedure the deviation between the K_I^d values observed in the experiments from pairs of bifocal caustics essentially reduce to within expected experimental scatter for the whole duration of loading. Thus it would appear that the main reasons for the observed experimental variation are accounted for by the three-dimensional elastodynamic simulation. Note that it is purely to highlight this point that the above "scaling" procedure was adopted. It is not the intention here to offer Fig. 9b as some kind of an empirical "correction curve" for experimental data.

Finally, as a matter of interest (for photoelasticity and the method of caustics in transmission), the radial variation of one typical stress component is shown in Fig. 11 for one particular time in the simulation and for different layers through the thickness. To bring out the effect of near-tip three-dimensionality, these are normalized by the corresponding two-dimensional full-field values. This figure points out the inadequacy of even a *full-field* two-dimensional analysis in characterizing the near-tip fields which are inherently three-dimensional.

CONCLUDING REMARKS

In this paper, preliminary results from an ongoing investigation regarding the domain of dominance of the two-dimensional elastodynamic asymptotic field were presented. It was shown that the assumption of K_I^d-dominance around the crack-tip might not always hold in experimental situations. Indeed it was shown that substantial variations could be obtained in what is purported to be an experimental measure of the dynamic stress-intensity factor because of this. It is felt that this fact must be taken into consideration in evaluating many of the experimental results in the literature. It must be pointed out that this problem is expected to also affect the interpretation of results from experiments using other techniques such as photoelasticity. This is because the underlying reason for lack of K_I^d-dominance is the interplay between *three-dimensional effects* and transient loading and, as such, it is not expected that any addition of higher-order terms to the two-dimensional asymptotic field (Dally *et al.*, 1985) would necessarily lead to a more accurate interpretation of experimental results. In conclusion, it seems that the assumption of an underlying K_I^d-dominant (or two-dimensional) field required for the interpretation of experimental data might not hold to a level of accuracy that would warrant many of the conclusions made in the literature regarding the accuracy of the crack-initiation toughness values as well as the uniqueness of $K_{ID} - \dot{a}$ relation or the specimen and acceleration dependence of the dynamic fracture toughness.

ACKNOWLEDGMENTS

Support of the Office of Naval Research through contract N00014-85-K-0599 is gratefully acknowledged. The computations were performed using the facilities of the San Diego Supercomputer Center and were made possible through an NSF-PYI grant MSM-84-51204 to the second author. The authors also want to acknowledge the contribution of Mr. R. Pfaff toward upgrading of the high-speed camera at GALCIT.

REFERENCES

Dally, J.W., W.L. Fourney and G.R. Irwin (1985). *Int. J. Fracture.*, 27, 159-168.
Freund, L.B. and R.J. Clifton (1974). *J. Elasticity*, 4, No. 4, 293-299.
Kalthoff, J.F. (1983). In: *Workshop on Dynamic Fracture,* (W.G. Knauss *et al.*, ed.), California Institute of Technology, 11-35.
Kobayashi, A.S. and S. Mall (1978). *Exp. Mech.*, 18, 11-18.
Kobayashi, T. and J.W. Dally (1980). In: *Crack Arrest Methodology,* (G.T. Hahn *et al.*, ed.), ASTM STP 711, 89-108.
Krishnaswamy, S. (1988). (doctoral dissertation), California Institute of Technology, Pasadena.
Manogg, P. (1964). (doctoral dissertation), Freiburg, West Germany.
Ravi-Chandar, K. and W.G. Knauss (1984). *Int. J. Fracture*, 25, 247-262.
Ravi-Chandar, K. and W.G. Knauss, (1987). *J. Appl. Mech.*, 54, 72-78.
Rosakis, A.J., (1980). *Engg. Fracture Mech.*, 13, 331-347.
Rosakis, A.J., J. Duffy and L.B. Freund, (1984). *J. Mech. Phys. Solids*, 32, 443-460.
Rosakis, A.J., and K. Ravi-Chandar (1986). *Int. J. Solids. Struct.*,22, No. 2, 121-134.
Rosakis, A.J., and A.T. Zehnder (1985). *J. Elasticity*, 15, No. 4, 347-368.
Takahashi, K. and K. Arakawa (1987). *Exp. Mech.*, 27, No. 2, 195-199.
Zehnder A.T. (1987). (doctoral dissertation), California Institute of Technology, Pasadena, California.

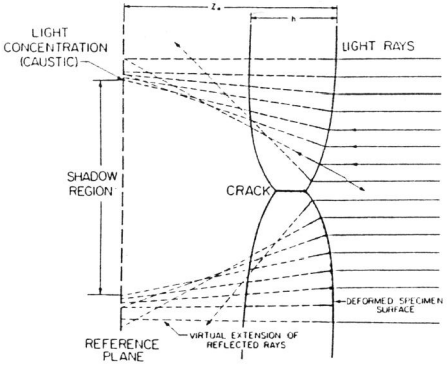

Fig. 1: Schematic of caustics in reflection.

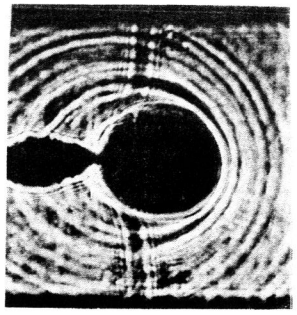

Fig. 2: Example of reflected caustic

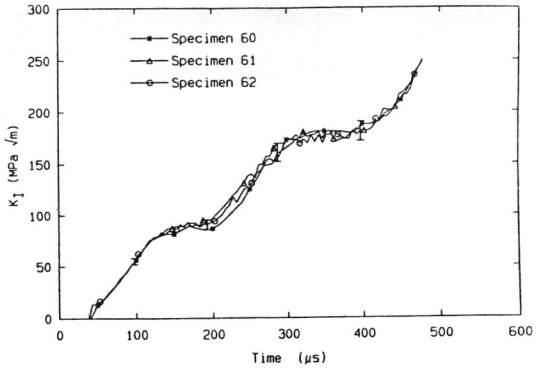

Fig. 3a: Scatter in experimental measurement: dynamically loaded stationary crack.

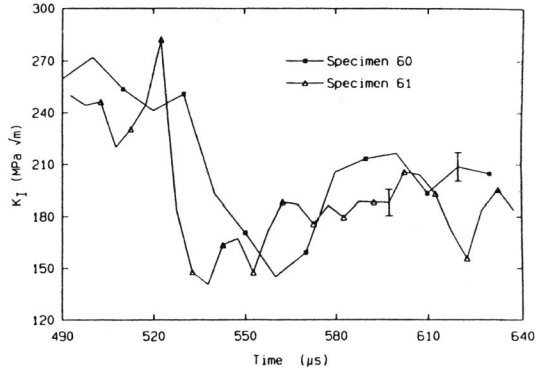

Fig. 3b: Scatter in experimental measurement: (b) dynamically propagating crack.

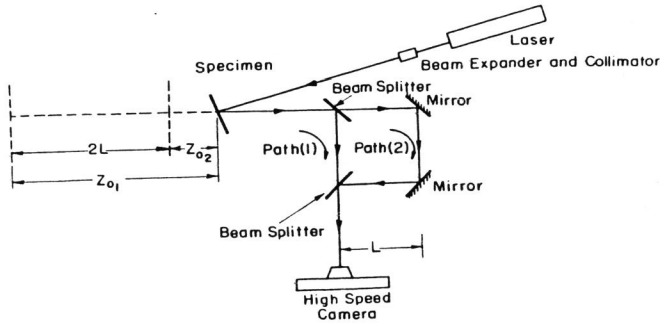

Fig. 4: Schematic of bifocal caustics set-up.

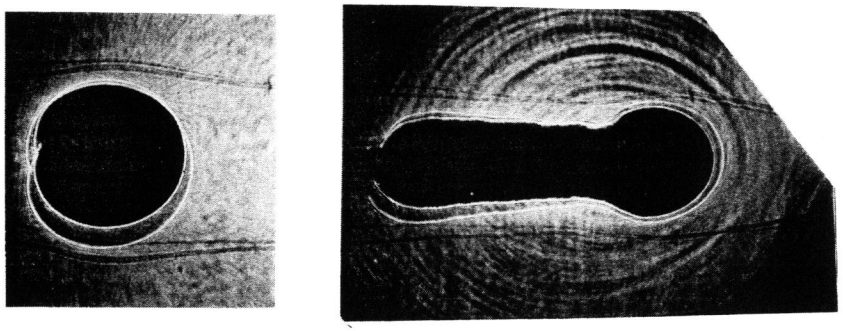

Fig. 5: Example of bifocal caustics for (a) stationary and (b) propagating cracks.

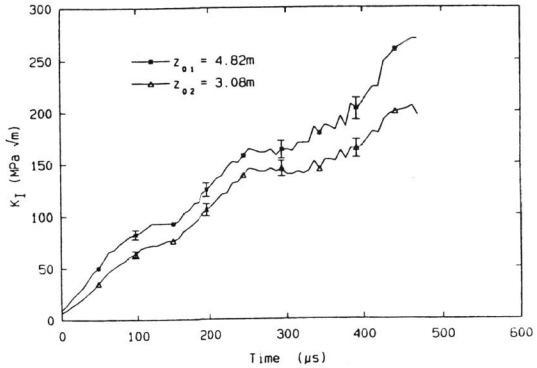

Fig. 6a: Results for specimen $\alpha - 3$: dynamically loaded stationary crack.

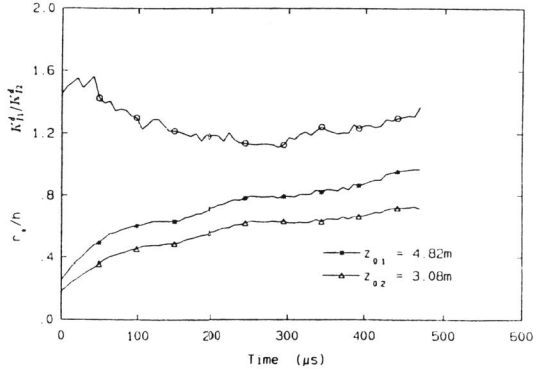

Fig. 6b: Results for specimen $\alpha - 3$: alternate representation.

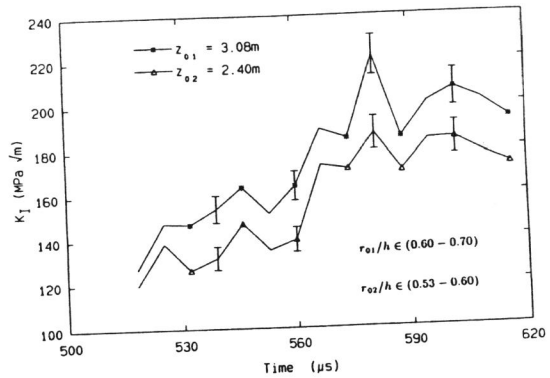

Fig. 7a: Results for dynamically propagating crack: (a) specimen $\alpha - 4$.

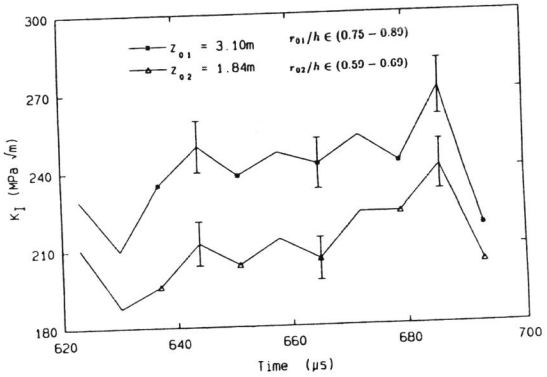

Fig. 7b: Results for dynamically propagating crack: (a) specimen $\alpha - 5$.

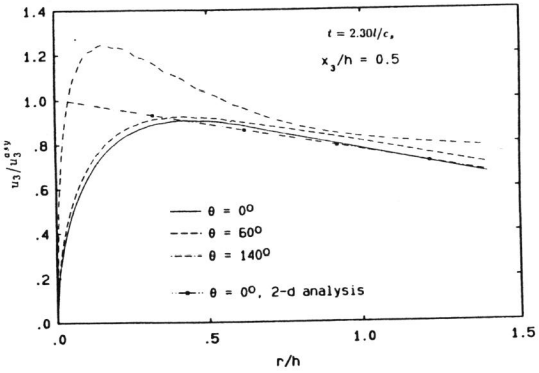

Fig. 8a: Radial variation of surface u_3 displacement

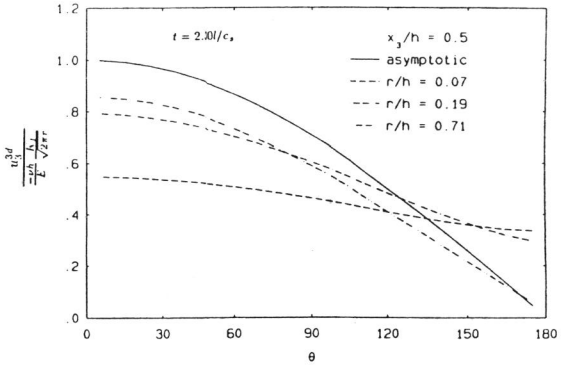

Fig. 8b: Angular variation of surface u_3 displacement

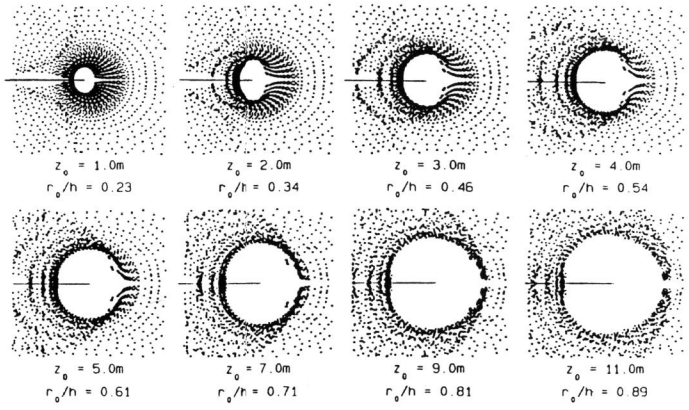

Fig. 9a: Example of numerically generated caustics.

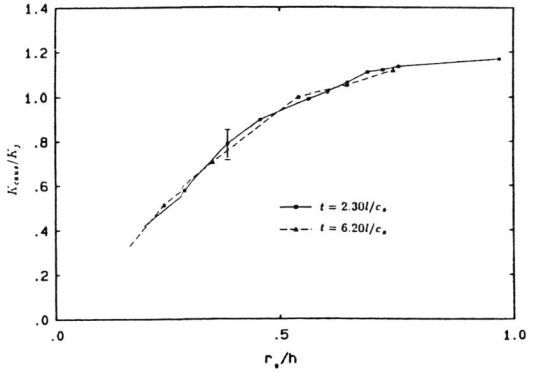

Fig. 9b: K_{caus}/K_j vs r_0/h from the three-dimensional simulation.

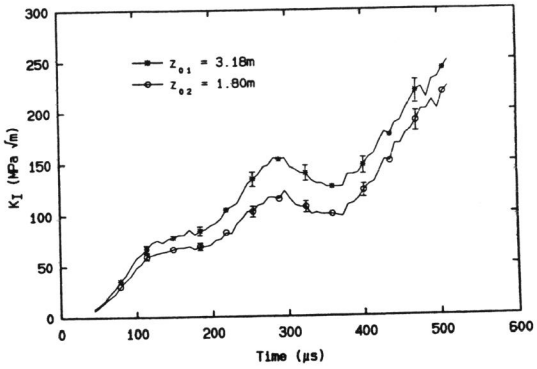

Fig. 10a: Experimental results for specimen 3q.

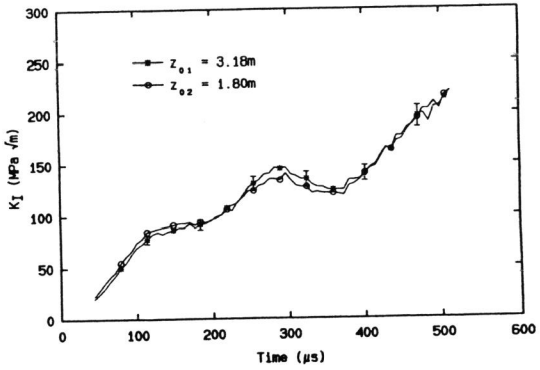

Fig. 10b: "Scaled" results for specimen 3q.

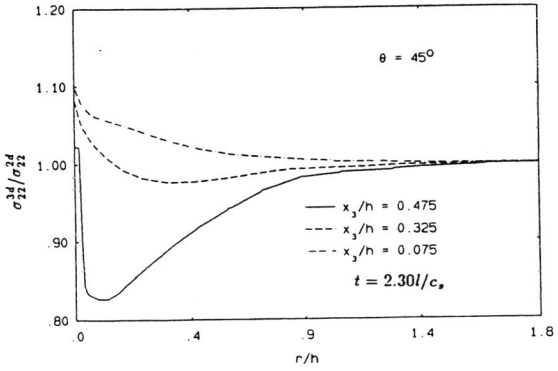

Fig. 11: Radial variation of $\sigma_{22}^{3d}/\sigma_{22}^{2d}$.